

Carbon Doped InP/InGaAs Heterojunction Bipolar Transistors Grown By MOCVD

P.M. DeLuca, B.E. Landini, and R.E. Welsler

Kopin Corporation, 695 Myles Standish Blvd. Taunton, MA 02780

Phone: (508) 824-6696, Fax (508) 824-6418, E-mail: pdeluca@kopin.com

R.L. Pierson, J.C. Li and B. Brar

Rockwell Scientific Corporation, 1049 Camino Dos Rios, Thousand Oaks, CA 91358

ABSTRACT

InGaAs/InP heterojunction bipolar transistors grown in a multi-wafer metal-organic chemical vapor deposition system will be demonstrated. Excellent large and small area DC and RF results are obtained for single and double heterojunction structures. The large area DC current gain was increased by a factor of 3 at a given base sheet resistance via growth optimization. DHBT devices exhibit a current gain cut-off frequency of $f_t \sim 125$ GHz and a unilateral gain cut-off frequency of $f_{max} \sim 125$ GHz.

INTRODUCTION

InP-based heterojunction bipolar transistors (HBTs) are being developed for 40 Gbps lightwave circuits and wireless applications. Compared to GaAs-based HBTs, InP/InGaAs HBTs have lower turn-on voltage and a higher frequency of operation. The dominant growth technology in InP production has been molecular beam epitaxy, which employs beryllium or carbon doping in the InGaAs base. Carbon-doped InP/InGaAs HBTs have demonstrated improved reliability in comparison with Be because carbon has a significantly lower diffusion rate in InGaAs [1]. The development of carbon-doped InP/InGaAs HBTs grown by metal-organic chemical vapor deposition (MOCVD) will accelerate the insertion of InP HBTs into reliable, commercial circuits in a cost-effective manner.

RESULTS AND DISCUSSION

InP HBT device wafers were grown using low pressure MOVPE in an Aixtron 2400 multiwafer production system. The layering

sequence (from the top surface) consisted of a highly doped n^+ -InGaAs contact layer, a 500 Å thick InP ($3 \times 10^{17} \text{ cm}^{-3}$) emitter, and a 400 - 1200 Å thick C-InGaAs ($2-3 \times 10^{19}$) base layer. This was followed by a 2000 Å thick InGaAs or InP ($1 \times 10^{16} \text{ cm}^{-3}$) collector and a 4000 Å thick InGaAs ($4 \times 10^{18} \text{ cm}^{-3}$) subcollector. Large area devices ($75 \mu\text{m} \times 75 \mu\text{m}$) were fabricated at Kopin using a simple wet-etching process and tested in the common base configuration using an HP4145 parametric analyzer. Small area devices were fabricated and tested at Rockwell Scientific Corporation.

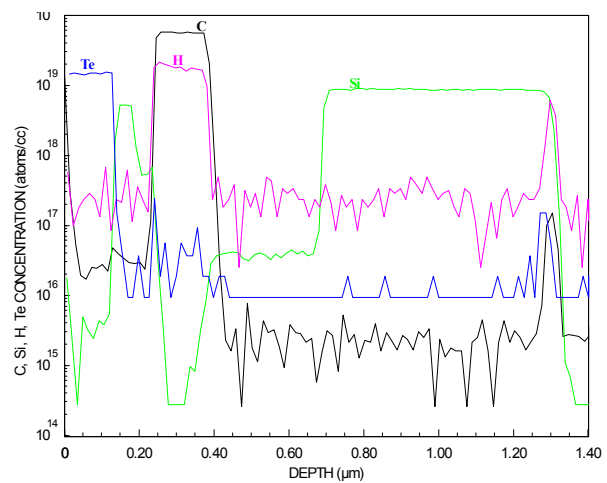


Figure 1: SIMS analysis plotting silicon, tellurium, carbon, and hydrogen concentrations versus depth in an InP/InGaAs HBT.

Figure 1 presents secondary ion mass spectroscopy (SIMS) results from a typical SHBT. The results are consistent with the structure defined above, indicating that well defined layers are present. Hydrogen passivation of the carbon in the InGaAs base has

been previously described by many groups [2]. The carbon concentration in the base is $\approx 6 \times 10^{19} \text{ cm}^{-3}$ and the hydrogen concentration is $\approx 2 \times 10^{19} \text{ cm}^{-3}$. This is consistent with the active carbon doping level estimated by R_{sb} and base thickness. Increasing the active carbon doping concentration in the base from $\approx 1 \times 10^{19}$ to $3 \times 10^{19} \text{ cm}^{-3}$ increased the hydrogen incorporation from $\approx 5 \times 10^{18}$ to $2 \times 10^{19} \text{ cm}^{-3}$. The SIMS results indicate that hydrogen passivation is increasing with carbon doping concentration, yet it remains at levels permitting acceptable device performance. The hydrogen concentration in carbon-doped InGaAs is similar to the concentration in MOCVD grown GaAs base layers. InGaP/GaAs HBTs grown by MOCVD have excellent reliability suggesting that the hydrogen concentration present in the InGaAs layers will not have an adverse affect on reliability [3].

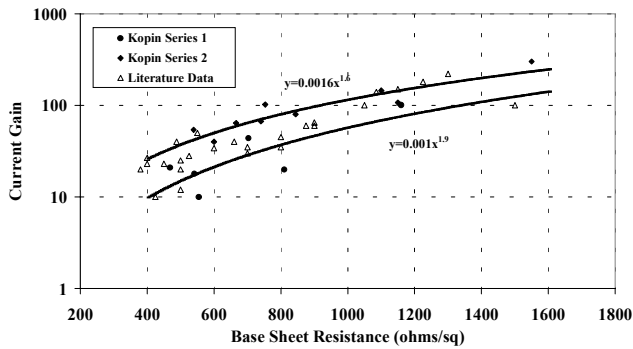


Figure 2: The DC current gain measured at 1 kA/cm^2 in large area devices ($L = 75 \mu\text{m} \times 75 \mu\text{m}$) as a function of R_{sb} (variable base thickness and doping). The solid line represents a power fit to the Kopin data sets. Representative data from the literature are included for reference [4]-[6].

Figure 2 plots the DC current gain (β) versus base sheet resistance (R_{sb}) at a collector current density $J_c = 1.0 \text{ kA/cm}^2$ for a series of InP HBTs with varying base thickness and doping levels. Within each series the base thickness and doping level is varied between $500 - 1100 \text{ \AA}$ and $2 - 3 \times 10^{19} \text{ cm}^{-3}$, respectively. A representative set of data from the literature is also presented for comparison [4]-[6]. The DC

current gain for all the samples appears to vary as a function of the square of the R_{sb} (solid line fit to Kopin data). This differs from GaAs-based HBTs, which exhibit a linear dependence on R_{sb} . Preliminary results suggest that base thickness, not base doping level, is responsible for the R_{sb} -squared dependence. The growth conditions in series 2 were optimized to maximize the DC current gain, resulting in a factor of 3 increase in the β for a given R_{sb} .

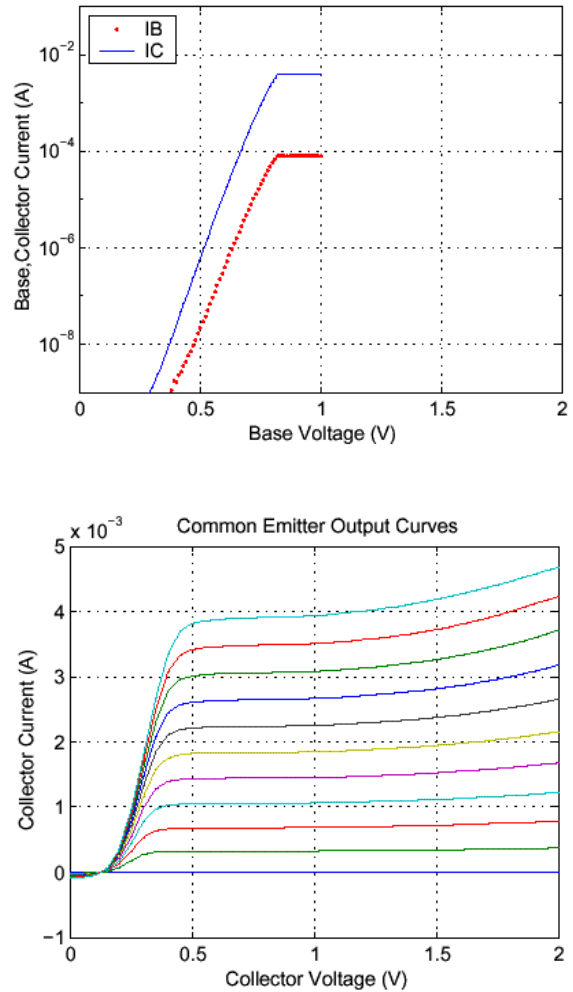


Figure 3: (a) Gummel plots from an InP SHBT small area device ($2 \times 4 \mu\text{m}^2$) with a $2 \times 10^{19} \text{ cm}^{-3}$ carbon doped base. The base thickness = 600 \AA and the $R_{sb} = 940 \text{ ohms/sq}$. (b) Output characteristics of the same device with a base current step of $4 \mu\text{A}$.

Figure 3 shows the gummel plots and common emitter characteristics of a typical SHBT small area device ($2 \times 4 \mu\text{m}^2$) with a 3000 \AA collector, a 600 \AA base and $R_{\text{sb}} = 940 \text{ ohms/sq}$ ($N_a \approx 2 \times 10^{19} \text{ cm}^{-3}$). The gummel plots are nearly ideal with no observed base leakage. The SHBT structure begins to breakdown under modest bias conditions, as expected. The RF properties of a similar SHBT structure with a 2000 \AA collector were measured on a $1 \times 10 \mu\text{m}^2$ device. The current gain cutoff frequency, f_t , and the power gain cutoff frequency, f_{max} , were measured at $>150\text{GHz}$ and 110 GHz , respectively, at a current density of $2 \times 10^5 \text{ A/cm}^2$.

The turn-on voltage (V_{be}), defined as the base-emitter voltage at a given collector current density, of an HBT is another important figure of merit. The turn-on voltage of InP/InGaAs HBTs has an added layer of complexity relative to GaAs HBTs due to the ternary InGaAs base layer. V_{be} is a function of the conduction band spike at the base-emitter interface, the base sheet resistance, and the band gap of the base layer [7]. Therefore, the composition of the InGaAs base layer, which determines the band gap, will alter V_{be} . Indium rich base layers will have a lower V_{be} while Ga rich layers will have a higher V_{be} , given similar base sheet resistance and conduction band spike heights. In order to properly compare turn-on voltages of different InP HBT structures the R_{sb} , base-emitter base conduction band height and composition of the base layer must be supplied.

Figure 4 shows the gummel plots and common emitter characteristics of an initial DHBT small area device ($1 \times 10 \mu\text{m}^2$) with a 3000 \AA collector, a 600 \AA base and $R_{\text{sb}} = 820 \text{ ohms/sq}$ ($N_a \approx 2.5 \times 10^{19} \text{ cm}^{-3}$). The DHBT structure was grown with minimal transition between the InP collector and InGaAs base. Again, the gummel plots are nearly ideal with no cross over indicated. The common emitter results are not as healthy as those of the SHBT, Fig. 3. The common emitter curves highlight the advantage and challenges of the InP DHBT structure. The knee voltage suggests that a

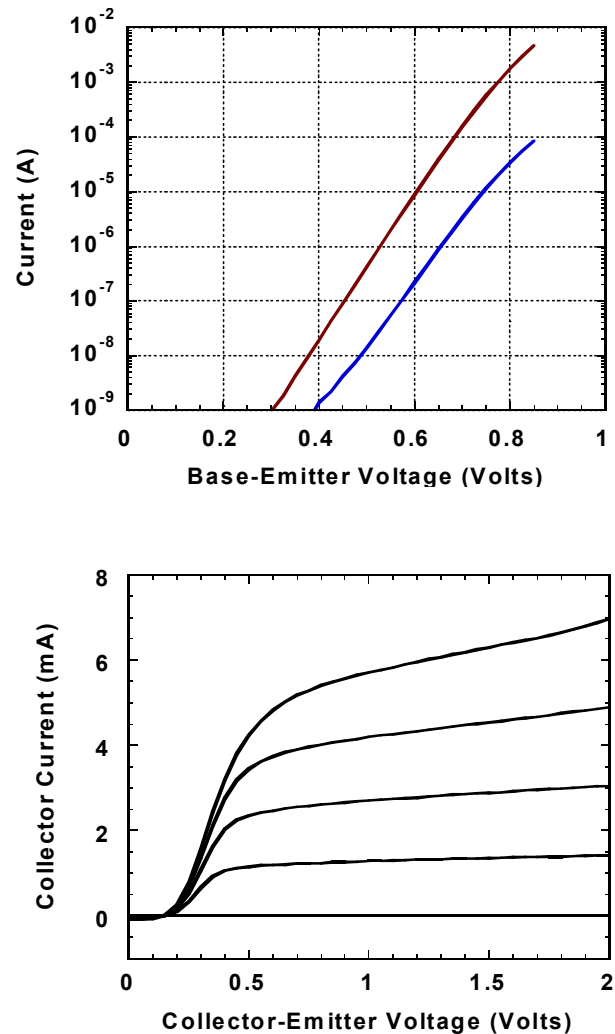


Figure 4: (a) Gummel plot from a $1 \times 10 \mu\text{m}^2$ InP DHBT with a 600 \AA base and $R_{\text{sb}} = 820 \text{ ohms/sq}$ ($N_a \approx 2.5 \times 10^{19} \text{ cm}^{-3}$). (b) Output characteristics of the same device with a base-current step of $4 \mu\text{A}$.

conduction band spike is present at the base-collector interface. However, unlike the DHBT, SHBTs show avalanche under modest bias. The current gain versus frequency at $1 \text{ mA}/\mu\text{m}^2$ is shown in Figure 5. The bias dependence of f_t and f_{max} is shown in Figure 6. RF characterization of this device measured an f_t and f_{max} of 125GHz . This was an initial effort at a DHBT with essentially no effort to suppress the base-collector conduction band spike. Improvements to the DHBT structure, such as thinning the base and collector, will improve the high frequency response of the device.

Additionally, minimizing the base-collector conduction band spike will allow the device to be driven at higher collector current densities, improving the frequency response of the DHBT. Further efforts to suppress the base-collector conduction band spike through the use of setback layers and linear grades are in progress.

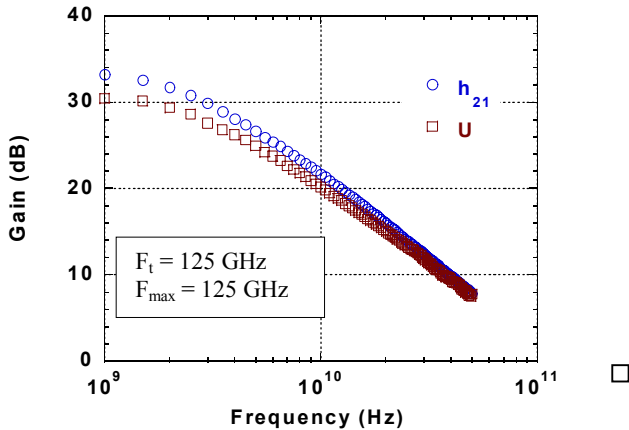


Figure 5: Current gain versus frequency for the device from Fig. 4. The current density is $1 \text{ mA}/\mu\text{m}^2$. F_t and F_{max} are extrapolated at -20 dB/decade .

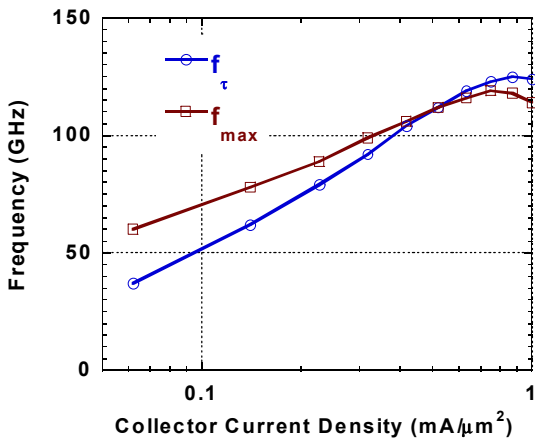


Figure 6: High-frequency dependence on collector current density of the DHBT shown in Fig. 4.

CONCLUSIONS

Carbon-doped InP/InGaAs HBTs with excellent large and small area DC and RF results have been grown in a multi-wafer MOCVD reactor.

Gummel plots from SHBT and DHBT exhibit nearly ideal behavior. The DC current gain has been shown to vary as a function of the square of the base sheet resistance. SHBT structures with an $f_t > 150 \text{ GHz}$ and DHBT structures with $f_t/f_{\text{max}} = 125 \text{ GHz}$ have been shown.

REFERENCES

- [1] S.R. Bahl *et al.*, "Be Diffusion in InGaAs/InP Heterostructure Bipolar Transistors," IEEE Electron Device Lett. vol. 21, pp. 332, 2000.
- [2] N. Watanabe *et al.*, "Hydrogen removal from C-doped InGaAs grown on InP by metalorganic chemical vapor deposition", Journal of Crystal Growth vol. 200, pp. 599, 1999.
- [3] N. Pan *et al.*, "High Reliability InGaP/GaAs HBT," IEEE Electron Device Lett. vol. 19, pp. 115, 1998.
- [4] J.-I. Song, "Chemical Beam Epitaxy Grown Carbon-Doped Base InP/InGaAs Heterojunction Bipolar Transistor Technology for Millimeter-Wave Applications," IEEE Trans. Electron Devices vol. E83, pp. 115, 2000.
- [5] W.K. Liu *et al.*, "MBE Growth of Large Diameter InP-Based Lattice-Matched and Metamorphic HBTs," 2001 IPRM Conference Proceedings, pp. 284, May 2001.
- [6] R.C. Gee *et al.*, "InP/InGaAs Double Heterojunction Bipolar Transistors Incorporating Carbon-Doped Bases and Superlattice Graded Base-Collector Junctions," Electron Lett. vol. 29, pp. 850, 1993.
- [7] R.E. Welser *et al.*, "Turn-On Voltage Investigation of GaAs-Based Bipolar Transistors with $\text{Ga}_{1-x}\text{In}_x\text{As}_{1-y}\text{N}_y$ Base Layers," IEEE Electron Device Lett. vol. 21, pp. 554, 2000.